Experimental and Numerical Investigation of Cylindrical and Shaped Cooling Holes with Forward and Reverse Injection.

Raj Gaurav[1], Ashutosh Kumar Singh[1], Kuldeep Singh[2], Dushyant Singh[3]*

[1]Department of Mechanical Engineering, National Institute of Technology Manipur, Imphal West, Manipur –795004, India.

[2]Gas Turbine and Transmission Research Centre, University of Nottingham, NG7 2TU United Kingdom

[3]Department of Mechanical Engineering, Dr B R Ambedkar National Institute of Technology Jalandhar, Punjab – India

***Corresponding author**: dushyant7raghu@gmail.com ; dushyants@nitj.ac.in

Abstract

The present work proposes a suitable injection hole configuration of cylinder and laidback fan-shaped with forward and reverse direction for film cooling of a gas turbine blades application, based on experimental and numerical analysis. The experimental study is conducted for cylindrical hole at blowing ratio (1), injection angle (35^o), and density ratio (1.2). The numerical study is performed for a wide range of operating parameters such as blowing ratios on (1-3), density ratios (2.42), mainstream flow Reynolds number as 4000 based on the hydraulic diameter of wind tunnel channel and, injection angle (35^o) with the effect of forward and reverse injection of laidback fan-shaped. The present study reveals that the formation of kidney vortices mitigated for reverse-shaped holes (secondary air is injected such that its axial velocity component is in the reverse direction to that of the mainstream) results in higher cooling performance with respect to forward-shaped holes. The

coolant coverage is likewise more consistent and higher in the lateral direction compared to the forward injection.

Introduction

To achieve high thermal efficiency and power output in the gas turbine engine based on the Brayton cycle, the gas turbine inlet temperature should increase to gain more thermal efficiency and power output. However, one of the significant consequences of the highly operated gas turbine inlet temperature is the potential failure of components in the turbine section due to heavy thermal load. To maintain a safe operating temperature, various cooling technologies have been suggested and reported by Han et al. [1]. One of the most important techniques for maintaining a lower temperature of these components is film cooling. It is a technology in which coolant gas is supplied as secondary air forming a thin layer on the surface that shields the components from high-temperature gas. Hole shape through which secondary air is injected, be it a cylindrical hole or shaped hole, diameter of the cooling hole, injection angle through which secondary air is injected, blowing ratio, density ratio, DR (ratio of the density of fluid of secondary stream to mainstream) and other geometric and operational characteristics affect film cooling performance.

Many authors have studied the effects of cylindrical and shaped holes experimentally and numerically [2-5]. Goldstein et al. [2] experimentally examined the impact of hole configuration on film cooling. They reported that the secondary flow with an expanded exit area decreases the mean velocity and results in lower mixing with the mainstream; as a result, the shaped hole shows promising results over the conventional cylindrical hole, and significant improvement in effectiveness is obtained. Andreopoulos & Rodi [4] accomplished an experimental investigation to study the jet in cross-flow. The study is performed at two velocities ratios (ratio of secondary stream velocity to the mainstream velocity), VR = 0.5 and 2, respectively. The study reveals that with a velocity ratio (0.5), the flow is partially inclined over the front part of the exit hole. However, at the higher velocity ratio (2), near the hole's exit, the jet is unaffected, and it penetrates the mainstream before it gets bent over. The consequences of hole geometry were investigated experimentally by Thole et al. [5], such as the cylindrical hole, fan shape, and laidback fan shape hole, on film cooling effectiveness and flow fields. The investigation is performed for DR=1, blowing ratio (M=1), the emphasis on the importance of jet formation inside the cooling hole, and distance and time of the peak turbulence levels, which tells the information about mixing the coolant with the mainstream. Saumweber & Schulz [6] studied the film cooling performance of cylindrical and fan-shaped holes at various boundary conditions for blowing ratio (0.5 to 2.5), injection angle (30°, 45°, and 60°), and constant DR= 1.75. They found an enhancement in the lateral spreading of secondary air using diffused exit-shaped holes. Park et al. [7] experimentally investigated that reverse injection had greater effectiveness and lateral coverage of the coolant stream in contrast to forward injection holes. Chen et al. [8] have done an Large eddy simulation study in the cross-flow at various blowing ratio depicting the relationship between heat transfer and the vortex evolution process. Shangguan [9] studied the effect of inclination angle on flow dynamics and heat transfer, as when the inclination angle is less than $45^{o,}$ more cooling is observed, showing weak strength of negative spanwise vorticity. Hou et al. [10] investigated the effect of inlet swirl on the leading edge film cooling.

Singh et al. [3] performed an experimental and numerical investigation on forward and reverse injection configurations. The studies were performed for blowing ratios (0.25 to 3.0), density ratio (0.9), and mainstream flow Reynolds number (Re = 3.75×10^5) using the characteristics dimension of the test section and injection angles (30°, 45°, & 60°). The formation of counter-rotating vortices is a significant issue in forward injection with a cylindrical hole, and reverse injection with the cylindrical hole is an efficient way to alleviate the kidney vortices. However, the reverse configuration with the shaped hole is still in the development phase in the available literature, which needs further exploration.

Based on the literature survey, most of the studies are mainly focused on different types of holes with varied operating parameters and injection angles for forward injections. Moreover, the effect of reverse injection with various operating parameters is not well understood for shaped holes. Hence, the film cooling study on the reverse-shaped hole needs further exploration.

The flow field and heat transfer characteristics of the forward laidback fan-shaped hole (FSH) and reverse laidback fan-shaped hole (RSH) are investigated in this study, based on experimental and numerical studies. The experimental study is conducted for cylindrical hole at M (1), injection angle (35^{o}), and DR=1.2. The numerical analysis is conducted for M (1-3), DR=2.42 and a mainstream Reynolds number of 4000 based on the hydraulic diameter of the mainstream inlet. The mainstream and secondary air turbulence intensities of 5% are considered. The secondary stream is injected at an angle of 35^{o} with the main flow for forward and reverse-shaped holes. The numerical simulations are also performed to obtain the flow pattern and quantitative trends of film cooling performance along with FSH and RSH.

Experimental Setup

Fig. 1 depicts the schematic arrangement of the experimental facility used in this work. The present experimental setup includes an open circuit wind tunnel system that provides mainstream flow, a coolant system providing secondary cooling air, and a test section with a flat plate having a film cooling hole indented on it. Both mainstream and secondary stream temperatures are measured with T-type thermocouples, whereas the surface temperature is measured with infrared thermography (using infrared Camera, FLIR A325). The mainstream flow velocity is measured with a pitot tube. Heaters are located at the entrance to the mainstream. The secondary air is cooled air stored in a double-stage reciprocating compressor. Then it is passed through the air filter and pressure regulator, which regulates the pressure of the secondary stream flow, and supplied into the plenum chamber through the mass flow controller (Alicat: MCR-3000SLPM-D-PAR).

The calibrations of instruments are done by following the previous work of [11]. Low thermally conductive material 'Plexiglass' (thermal conductivity, $k_p < 0.16$) makes the test plate 12mm thick, and the plate is well insulated from ambient using a thick coating of glass wool and styrofoam sheets on it so that it can be considered an adiabatic condition.

Experimental Procedure

In the case of the present experiment, the mainstream is heated air, and the secondary stream of coolant is at a relatively lower temperature. The dimensions of the plate taken for the experimental study are represented in Fig. 2 (a). The mainstream flow temperature is measured with the help of T-type thermocouples placed upstream of the test plate. Similarly, the secondary stream air temperature is measured using a thermocouple placed in the plenum chamber, as shown in Fig. 2 (b). The film cooling surface is coated with matt-finished black paint to obtain high surface emissivity (0.95). The surface temperature is recorded with an Infrared Camera to assess film cooling performance over the plate. Before the data collection, the mainstream and secondary stream supply is switched on at pre-set velocity.

In the present study blowing ratio is defined as the ratio of mass flux of the secondary stream to the mainstream flow, which is expressed as:

$$M = \frac{\rho_{sec} u_{sec}}{\rho_{ms}\, u_{ms}} \quad (1)$$

u_{ms} and u_{sec} are mainstream and secondary stream velocity, respectively, whereas ρ_{ms} and ρ_{sec} are mainstream density, and secondary-stream density, respectively. Density ratio is defined as the ratio of the density of the secondary stream to the mainstream, as:

$$\rho = \frac{\rho_{sec}}{\rho_{ms}} \quad (2)$$

The expression for calculating the film cooling effectiveness is given as:

$$\eta = \frac{T_{ms} - T_{wx}}{T_{ms} - T_{sec}} \quad (3)$$

Where T_{ms} is the temperature of heated mainstream, T_{sec} is secondary stream temperatures and T_{wx} is the flat plate wall temperature along the x direction. The repeated measurements ensure that the data taken is at a comparable steady-state condition. For mainstream flow, the data taken 1 hour after turning on the heater (dT=0.1 ^{o}c from centre to corner & dT/dt=0.005 ^{o}c/minute) was used for the present study before that was used as a reference to study the behaviour of data changes. Similarly, the secondary streamflow takes 45 minutes to attain the steady-state temperature (dT=0.1 ^{o}c from top to bottom in the plenum chamber & dT/dt=0.002 ^{o}c/minute) turned on. Once the flow and heat transfer conditions reach the static state, the data recording is performed.

The uncertainty in the effectiveness of the present study is calculated using Eq. (4), based on the approach described by Kilne and McClintock [12], Where T_{ms}, $T_{sec,}$ and T_w represent the mainstream, secondary stream, and surface temperature, respectively. For the present experimental study, T_{ms} is 333K, T_{sec} is 303K with an uncertainty of ±1K, and the uncertainty of the Infrared Camera is ±0.5K. The overall uncertainty in film cooling effectiveness at a 95% confidence level is ±11%. A brief Detail of instruments measurement uncertainty in the present experimental study is given in table 1.

$$\Delta\eta = \sqrt{\left(\frac{\partial\eta}{\partial T_{sec}}\Delta T_{sec}\right)^2 + \left(\frac{\partial\eta}{\partial T_{ms}}\Delta T_{ms}\right)^2 + \left(\frac{\partial\eta}{\partial T_w}\Delta T_w\right)^2} \quad (4)$$

Numerical model

The present numerical simulation is carried out using commercial software ANSYS Fluent 2020 R1 [13] to investigate the performance of film cooling and flow characteristics of the FSH and RSH. The numerical models having a computational domain of length 40D, width 6D, and height 10D are used to observe the effect of coolant in the downstream upto X/D=30 and to study the effect of jet penetration of secondary air, height is taken sufficient as 10D. A shaped hole located at 10D downstream of mainstream flow for both FSH and RSH. The secondary stream is supplied from a cubical plenum of length 5D, represented in Fig. 3 (a) (b) & (c), respectively. The cross interaction of mainstream and secondary stream indicates a higher strength of the turbulent mixing effect, close to the edge of the film cooling hole; hence this flow is considered to be turbulent.

In present simulations, the governing equation of mass momentum and energy are solved by assuming flow to be steady, incompressible and turbulent. The governing equations of mass momentum and energy are stated in Eqs (5)-(7).

$$\frac{\partial(\rho u_i)}{\partial X_i} = 0 \quad (5)$$

$$\left(\frac{\partial(\rho u_i u_j)}{\partial X_j}\right) = -\frac{\partial p}{\partial X_j} + \frac{\partial}{\partial X_j}\left[\mu\left(\frac{\partial(u_i)}{\partial X_i} + \frac{\partial(u_j)}{\partial X_i}\right) - \rho\overline{u'_i u'_j}\right] \quad (6)$$

$$\frac{\partial \rho u_j T}{\partial \mathrm{X}} = \frac{\partial}{\partial X_j}\left(\frac{\mu}{\mathrm{Pr}}\frac{\partial T}{\partial X_j} - C_p\overline{u'_j T'}\right) \quad (7)$$

Where u and u' signifies the mean and fluctuating components of velocity, p is pressure, ρ is density, T is temperature, μ is the dynamic fluid viscosity, X is coordinate, and the subscripts i and j denote the directions used in the cartesian coordinates system. The term $\rho\overline{u'u'_J}$ is known as the Reynolds stress term, and the term $C_p\overline{u'_J T'}$ indicates the specific turbulence heat fluxes; to solve Eq. (6), the Reynolds stresses term has to be modeled. The Boussinesq approximation is employed to estimate the Reynolds stresses term. Similarly to solve Eq.(7), the specific turbulence heat fluxes flux term is calculated using the eddy diffusivity model. For the closure of the Reynolds stress term, the k-ε (Realizable) is employed, based on suggestions of the previous studies [14] .A detailed description of the Reynolds Average Navier Stokes (RANS) models is presented in [15].

Boundary Conditions

The mainstream inlet is assigned as the velocity inlet boundary condition with a velocity of 128m/s and the secondary stream velocity is changed depending upon the value of the blowing ratio, and the respective temperature for both the streams is also assigned. The outlet boundary is treated as the pressure outlet with a zero-pressure gauge, and the walls are adiabatic. A brief detail of operating parameters and boundary conditions are given in Table 2 and Table 3 respectively.

The Fluid Properties

Both mainstreams are heated air, while the secondary stream is relatively cold air. The temperature difference in the region is significant, so the variation in the physical properties of air with temperature is considered for the present study. Turns [16] suggested that a fourth-order polynomial mentioned in Eq. (8)– (10) is used for specific heat, dynamic viscosity and thermal conductivity respectively, while the density is calculated using local fluid temperature. All the properties are valid in the temperature range of 100 K - 2300 K.

Specific heat, (C_p) J/kg.K

$$C_p = (9.08 \times 10^{-11})T^4 - (4.80 \times 10^{-7})T^3 + (8.073 \times 10^{-4})T^2 - 0.321T + 1.04 \times 10^3 \quad (8)$$

Dynamic viscosity (μ), Pa.s

$$\mu = (1.70 \times 10^{-14})T^3 - (4.04 \times 10^{-11})T^2 + 6.85 \times 10^{-8}T + 1.06 \times 10^{-6} \quad (9)$$

Thermal conductivity (K_{th}), W/m.K

$$K_{th} = (7.9 \times\times 10^{-12})T^3 - (2.40 \times 10^{-8})T^2 + (8.3 \times 10^{-5})T + (2.8 \times 10^{-3}) \quad (10)$$

Grid Independency Test

Figure 4 compares different grids to obtain the grid-independent solution for forward circular hole, where four different grid sizes were considered. All four grids follow the same trends, and no significant changes were observed beyond of 3,69, 890 total cells, hence it is taken for further study to reduce the computational cost. However, the numerical result follows the trends of experimental variations, and hence it can be used for further study.

Results and Discussion

To access the film, cooling characteristics of both forward and reverse configurations are compared. The numerical results of centreline effectiveness (η_{cl}) and local lateral film cooling effectiveness (η_{la}), along with the effectiveness contours at various locations, are also discussed for FSH and RSH.

Film cooling validation

Experimental results on a flat plate for M = 1 and DR = 1.2 at a 35° injection angle validate the present numerical model. The grid topology of the computational domain for the reverse-shaped hole is shown in Figure 5.

Two equation RANS (i.e., k-ε-Realizable) model is used to predict the film cooling flow over flat surface. To validate the numerical methodology, the model is validated against the in-house set of experiment as well as the available experimental data of Singh et al. [11] and Sinha et al. [17]. The test case has been performed for M = 1, and DR = 1.2 at fixed injection angle of 35°, and the centerline effectiveness is plotted for comparisons. The experimental measurement along with its uncertainty have been presented in the downstream direction of X/D = 0 to 12. The plot in Fig.6 clearly indicate that numerical model follows experimental trends of variations. However, the numerical results show closer agreement with Sinha et al. [17], the model well predict the near hole regions however, a maximum deviation of 40% (overprediction of 0.08 with respect to experimental data 0.12) is reported in far downstream location at X/D=11.7. The numerical model well predicts in critical domain (i.e., cross-flow region near hole) therefore model is considered suitable for further studies.

Centreline Effectiveness

The centreline film cooling effectiveness variation for forward and reverse-shaped holes in the direction downstream of the hole are compared at various M =1, 2, and 3, as shown in Fig. 7. The centreline effectiveness is measured from the rare ends of the cooling hole footprint (i.e., X/D = 0) to the downstream. Fig. 7 clearly shows that the FSH performance is significantly higher than the RSH near the hole region, i.e., X/D (2 to 4) for blowing ratio (1 to 2). The contours shown in Fig. 8 (a) and 9 (a) clearly show that the coolant flow is more skewed along the centreline for the FSH than the RSH. Therefore, the performance of the forward centreline effectiveness is better. The centreline effectiveness of FSH is 8.27% higher than that of the RSH at X/D = 0 at the M=1. The centreline effectiveness of FSH is higher up to X/D =1.5, and after that, RSH shows better performance. Similarly, at M=2, the centreline effectiveness for FSH is higher till X/D=8, and further downstream, RSH shows better performance. For the M = 3, RSH shows better effectiveness than FSH (X/D=0 to X/D=25). It is also observed that increasing the blowing ratio at a fixed density ratio leads to more penetration of coolant in the jet for FSH than RSH and hence more mixing with the mainstream flow. Figure 8-9 (b) – (e) shows the flow streamline contours of dimensionless temperature (θ) for FSH and RSH, respectively, at M = 2. The formation of kidney vortices significantly influences the film cooling performance. Therefore, various planes are considered to study the formation of kidney vortices and their effect on flow and film cooling. Fig. 8 (b) represents the midplane (X-Y plane) taken along the centreline, indicating that the secondary stream entered the mainstream region and was suppressed toward the plate due to the mainstream flow. Fig. 8 (c) - (d) shows the streamlined plot in-plane normal to mainstream (Y-Z) at X/D = 2, 10, respectively. This figure shows the formation of a kidney vortex with anti-kidney pair, and it is also observed that the strength of the anti-kidney pair increases downstream at X/D =10. The coolant spread is shown in Fig. 8 (e) by taking a plane one node above the flat plate, i.e., at Y/D = 0 (X-Z plane). It can be observed that the secondary stream spread in the lateral direction is limited to the hole footprints. Fig. 9 (b) represents a non-dimensional temperature contour along the mid-plane taken along the centreline, i.e., at Z/D=0 (X-Y plane), the contour clearly shows that the secondary stream entered the mainstream region and was suppressed toward the plate due to the mainstream flow. Fig.9 (c) - (d) shows the streamlined plot in the plane normal to mainstream (Y-Z) at X/D=2, 10, respectively, for the reverse-shaped hole. Fig. 9 (e) shows the coolant spread in the lateral direction of a flat plate, i.e., X-Z plane one node above the flat plate, i.e., X-Z plane at Y/D = 0. The horizontal vortex pair can also be observed at Y/D = 0.5 and further diminished and trapped below Y/D=1.5.

Local Lateral Film Cooling Effectiveness

Fig.10 compares the local effectiveness trends in the spanwise direction at various M = 1-3. The shaped hole configurations are compared at X/D =5 and 10. It can be observed that the lateral spreading of the coolant in the case of RSH is higher than the FSH at all blowing ratios taken for the present study. In FSH, secondary fluid is more accumulated along the centreline. The same phenomenon can also be observed from the contours mentioned in Fig. 8 (a) & 9 (a).

Conclusions

The film cooling performance of laidback fan-shaped holes is investigated for the forward and reverse injections at different M =1-3 with an injection angle of 35^o. Based on the present study, the following inferences can be drawn:

- At the M = 1, the maximum enhancement in effectiveness with RSH is 7.8% at X/D=6, whereas at a higher blowing ratio of 3, the effectiveness of RSH is 37.08% higher than that of FSH at X/D=14. The reverse-shaped hole has higher effectiveness than a forward-shaped hole at a higher blowing ratio and is comparable at the lower blowing ratios stating that the reverse-shaped hole can provide better cooling as compared to the forward one for the laidback fan-shaped hole.
- RSH flow displaced the vortices far from the centerline plane to enable the coolant flow to distribute in the spanwise direction. Thus, the lateral spreading of the secondary fluid for RSH can be seen as more uniform than FSH at all blowing ratio taken for the present study, whereas for FSH, it is skewed towards the centre.
- With the increase in the blowing ratio, there is a decrease in effectiveness for both FSH and RSH.

- The flow study suggests that kidney vortices are apparent in the case of forward injection at all the injection angles. Kidney vortices are not produced in the case of reverse holes, which give greater adhesion for the coolant flow to the surface than for the forward injection; consequently, greater film cooling is seen.
- Investigation of the secondary-stream exit condition indicated that the blowing ratio, the type of injection, and the hole geometry had a substantial influence on flow variables in the secondary-stream exit plane.

Acknowledgment

The authors are thankful to Science and Technology (SERB), New Delhi under Core Research Grand; Project Ref. No. CRG/2021/001213; for the experimental and computational facility to carry out the present study in the Department of Mechanical Engineering at NIT Manipur, India.

Nomenclature	
C_p	Specific heat, J/kg K
D	Hole injection diameter, m
DR	Density ratio, $\frac{\rho_{sec}}{\rho_{ms}}$
i,j,and k	Unit vectors in X,Y and Z direction respectively
I	Turbulent intensity
k	Turbulent kinetic energy, m^2/s^2

k_p	Thermal conductivity of test plate, W/m K
k_{th}	Thermal conductivity, W/m K
M	Blowing ratio, $\frac{\rho_{sec} u_{sec}}{\rho_{ms} u_{ms}}$
P	Pressure, N/m^2
t	Time, sec
T	Absolute temperature, K
u	Velocity, m/s
u'	Fluctuating velocity, m/s
VR	Velocity ratio, $\frac{u_{sec}}{u_{ms}}$
X,Y,Z	Coordinates in X,Y and Z directions respectively
Greek Symbols	
η	Film cooling effectiveness, $\frac{T_{ms}-T_{wx}}{T_{ms}-T_{sec}}$
θ	Non-dimensionless temperature, $\frac{T_{ms}-T}{T_{ms}-T_{sec}}$
μ	Dynamic viscosity, Pa.s
ρ	Density, Kg/m^3

ε		Turbulent dissipation rate, m^2/s^3
Subscripts		
cl	centreline direction	
la	lateral direction	
ms	mainstream	
sec	secondary	
wx	wall X direction	
Acronyms		
FSH		Forward laidback fan-shaped hole
RANS		Reynolds averaged Navier stokes equation
RSH		Revere laidback fan-shaped hole

References

[1] J. C. Han, S. Dutta, and S. Ekkad, *Gas Turbine Heat Transfer and Cooling Technology*, 2nd ed., CRC Press, 2012.

[2] R. J. Goldstein, E. R. G. Eckert, and F. Burggraf, "Effects of hole geometry and density on three-dimensional film cooling," *Int. J. Heat Mass Transf.*, vol. 17, no.5, pp. 595-607, May 1974. DOI: 10.1016/0017-9310(74)90007-6.

[3] K. Singh, B. Premachandran, and M. R. Ravi, "Experimental and numerical studies on film cooling with reverse/backward coolant injection," *Int. J. Therm. Sci.*, vol. 111, pp. 390–408, Jan. 2017. DOI: 10.1016/j.ijthermalsci.2016.09.027.

[4] J. Andreopoulos and W. Rodi, "Experimental investigation of jets in a cross-flow," *J. Fluid Mech.*, vol. 138, pp. 93–127, 1984. DOI: 10.1017/S0022112084000057.

[5] K. Thole, M. Gritsch, A. Schulz, and S. Wittig, "Flowfield measurements for film-cooling holes with expanded exits," *Proc. ASME- Int. Gas Turb. Aero. Cong. Exh.*, vol. 4, pp. 96-GT-174, June, 1996. DOI:10.1115/96-GT-174.

[6] C. Saumweber, and A. Schulz, "Free-stream effects on the cooling performance of cylindrical and fan-shaped cooling holes," *Proc. ASME - Turbo Expo*, vol. 4, pp. 879-891, June, 2008. DOI:10.1115/GT2008-51030.

[7] S. Park, E. Y. Jung, S. H. Kim, S. H., Sohn, H. S. Sohn, "Enhancement of film cooling effectiveness using backward injection holes," *Int. J. Therm. Sci.*, vol. 110, pp. 314–324, Dec. 2016. DOI: 10.1016/j.ijthermalsci.2016.08.001.

[8] Z. Y. Chen, J. M. Zhan, C. W. Li, W.Q. Hu and Y. J. Gong, "The effect of vortex shedding in film-Cooling processes," *Heat Transf. Eng.*, vol. 42, no. 17, pp. 1432-1451, Jul. 2020. DOI: 10.1080/01457632.2020.1800260.

[9] Y. Shangguan, "Large-Scale numerical investigation of coherent structure dynamics in film cooling, *Heat Transf. Eng.*, vol. 43, no. 8-10, pp. 830-845, Mar. 2021. DOI: 10.1080/01457632.2021.1906508.

[10] R. Hou, F. Wen, Y. Luo and S. Wang, "Influence of inlet swirl on film cooling of the turbine leading edge, *Heat Transf. Eng.*, vol. 42, no. 2, pp. 985-1001, May. 2020. DOI: 10.1080/01457632.2020.1766247.

[11] K. Singh, B. P. M. R. Ravi, and M. R. Ravi, "Experimental assessment of film cooling performance of short cylindrical holes on a flat surface," *Heat Mass Transf.*, vol. 52, no. 12, pp. 2849–2862, March 2016. DOI: 10.1007/s00231- 016-1777-6.

[12] S. J. Kline and F. M, "Describing uncertainty in single sample experiments," *Mech. Eng.*, vol. 75, pp. 3–8, 1953.

[13] *ANSYS Fluent-2020R1 User Guide*, Canonsburg, 2020.

[14] K. Singh, B. Premachandran, and M.R. Ravi, M.R., “A numerical study on the 2D film cooling of a flat surface”. *Numer. Heat Transf. A*, Vol. *67*, No. 6 pp.673-695,2015. DOI: 10.1080/10407782.2014.949131.

[15] D. Singh, B. Premachandran, and S. Kohli, “Numerical Simulation of the Jet Impingement Cooling of a Circular Cylinder.” *Numer. Heat Transf. A*, Vol. 64, No. 2, pp. 153–185,2013. DOI:10.1080/10407782.2013.772869.

[16] S. Turns, *Thermal-Fluid Sciences-An Integrated Approach*, Cambridge University Press: New York, 2006.

[17] A. K. Sinha, D. G. Bogard, and M. E. Crawford, “Film-cooling effectiveness downstream of a single row of holes with variable density ratio,” *J. Turbomach.*, vol. 113, no. 3, pp. 442-449, Jul. 1991. DOI: 10.1115/1.2927894.

List of Tables

Table:2	Operating parameters for present numerical study for FSH and RSH.
Table:3	Boundary conditions considered in the present numerical study

Table 1:

Instrument	Uncertainty
Infrared Camera	±1K
Thermocouple	±0.5K
Pitot Tube	±0.3%
Mass Flow Controller	±0.8%

Table 2:

Parameters	Range
Re_{ms}	4000
Blowing ratio (M)	1, 2 and 3
Density ratio (DR)	2.42

T_{ms} (K)	1561
T_{sec} (K)	644
Turbulent Intensity (I)	5%

Table 3.

Specific position in Computational domain	**Boundary Type**	
	Fluid condition	**Temperature condition**
Mainstream inlet	Velocity inlet (128m/s) Turbulent intensity (5%)	1561K

Secondary stream inlet	Velocity inlet depends on blowing ratio	644K
Walls	No-slip	No heat flux (adiabatic-wall)
Mainstream outlet	Outlet	

List of Figures

Fig. 8 FSH streamlines colored at M= 2 (a) effectiveness downstream at Y/D = 0 (XZ Plane); dimensionless temperature(θ): (b) Z = 0 (XY plane) (c) X/D = 2 (YZ Plane) (d) X/D =10 (YZ Plane) (e) Y/D = 0 (XZ Plane).

Fig. 9 RSH streamlines colored at M=2 (a) effectiveness downstream at Y/D =0 (XZ Plane); dimensionless temperature(θ): (b) Z = 0 (XY plane), (c) X/D =2 (YZ Plane), (d) X/D =10 (YZ Plane), and (e) Y/D = 0 (XZ Plane).

Fig. 10 Comparison of centerline film cooling effectiveness with X/D for the FSH & RSH hole for various blowing ratios.

1	Compressor	7	Secondary air	13	IR Camera
2	Pressure indicator	8	Plenum	14	Static Pitot Tube
3	Control valve	9	Thermocouple	15	Manometer
4	Filter	10	D A Q	16	Pump
5	Pressure regulator	11	Computer	17	Control
6	Mass flow controller.	12	Test plate	18	Heater rod

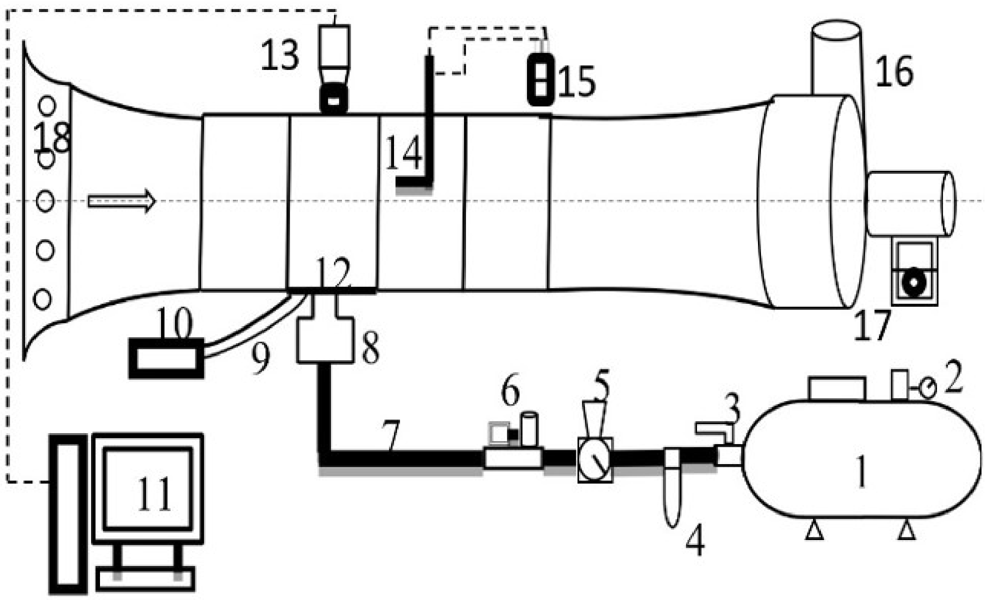

Fig. 1 Schematic Experimental setup

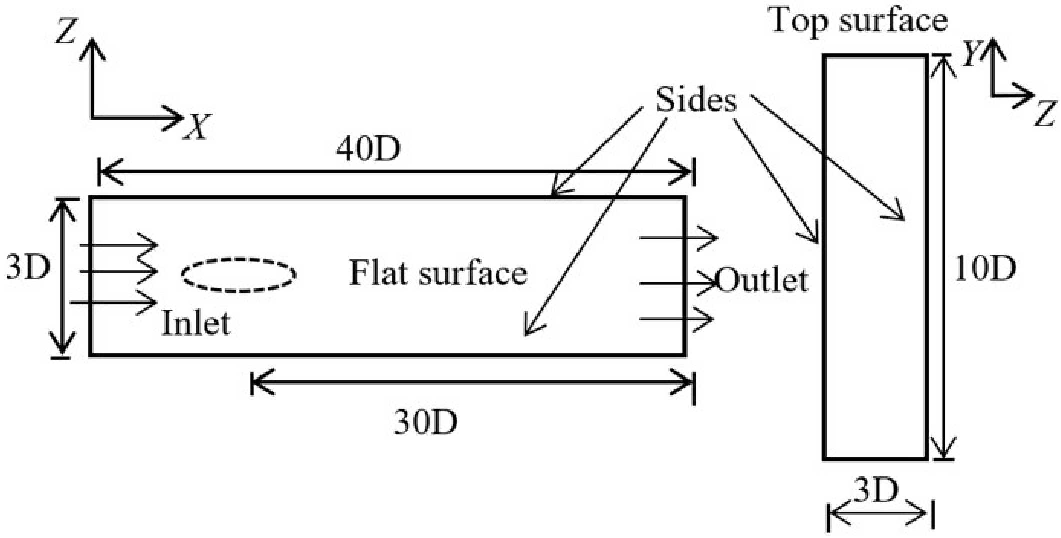

(a)

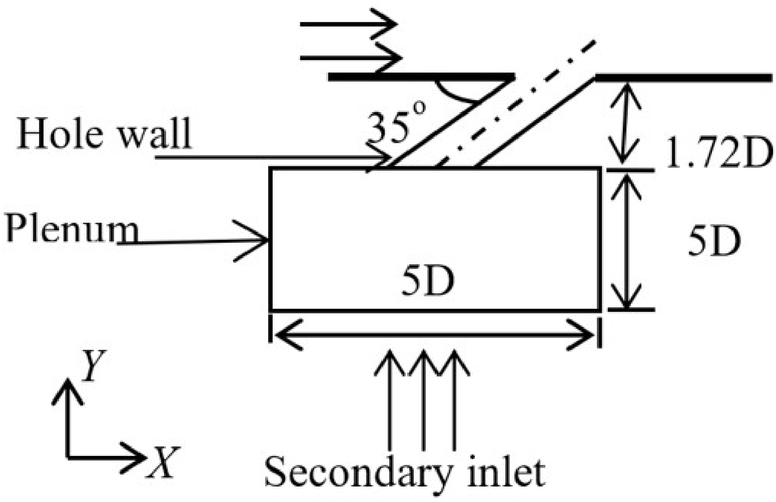

(b)

Fig. 2(a) Dimension of the hole and plate (b) Cooling hole arrangement on the test plate.

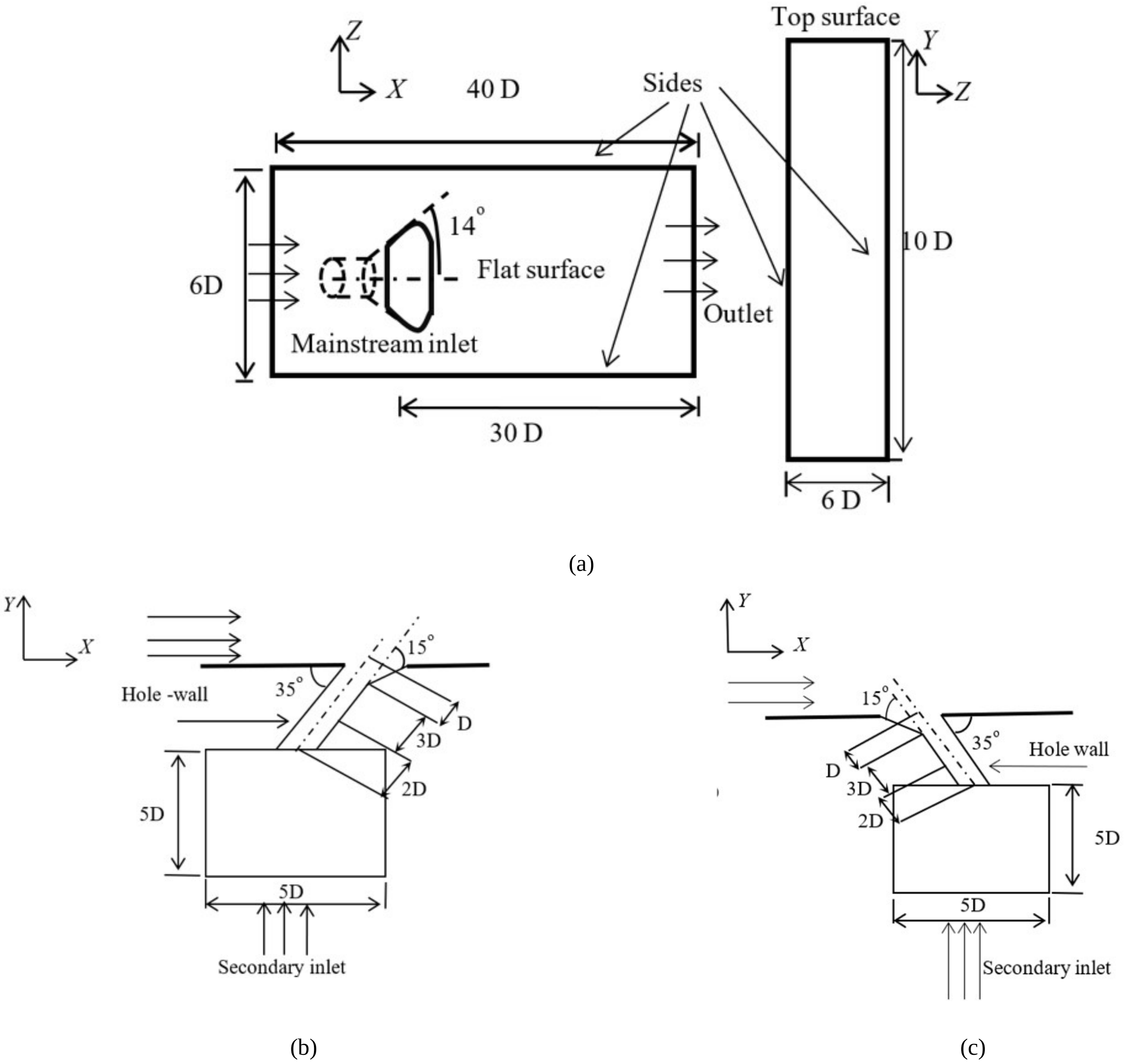

Fig. 3(a) Dimension of the shaped hole and test plate and Cooling hole arrangement for (b) FSH (c) RSH

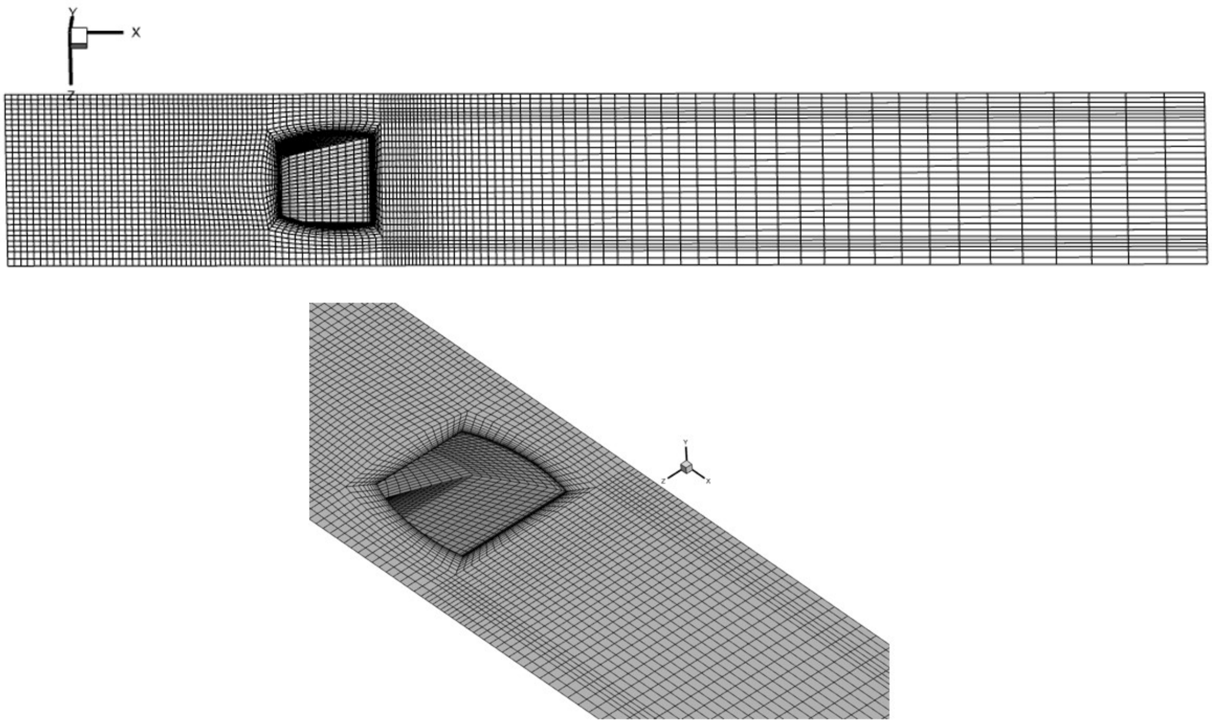

Fig. 4 Grid topology of the computational domain

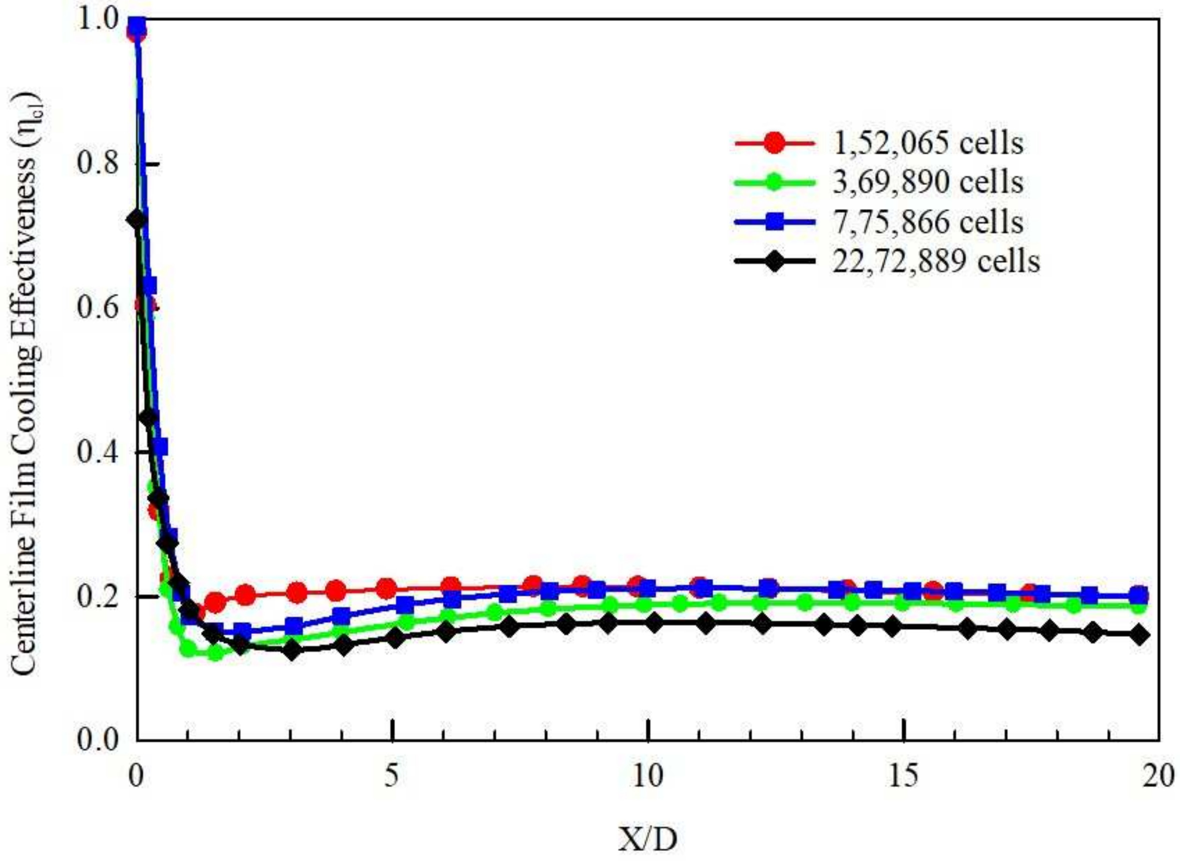

Fig. 5 Grid independence study for the forward cylindrical hole.

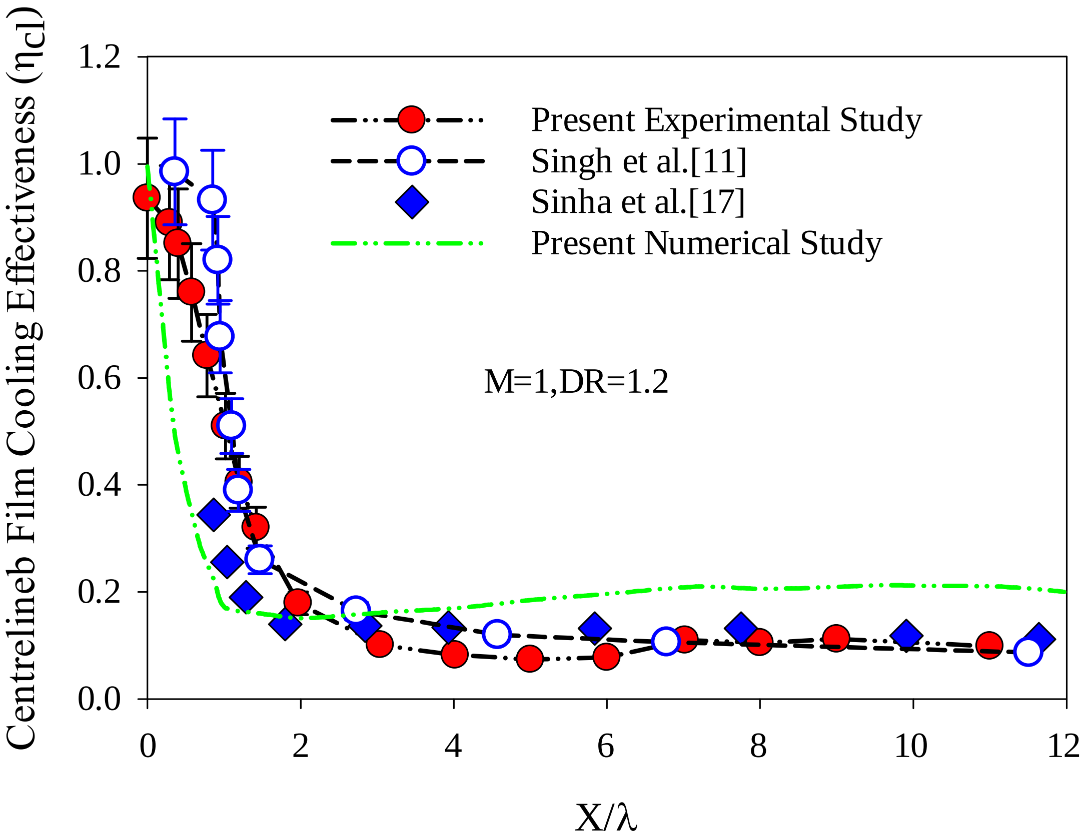

Fig. 6 Comparison of centerline film cooling effectiveness with X/D for the cylindrical hole.

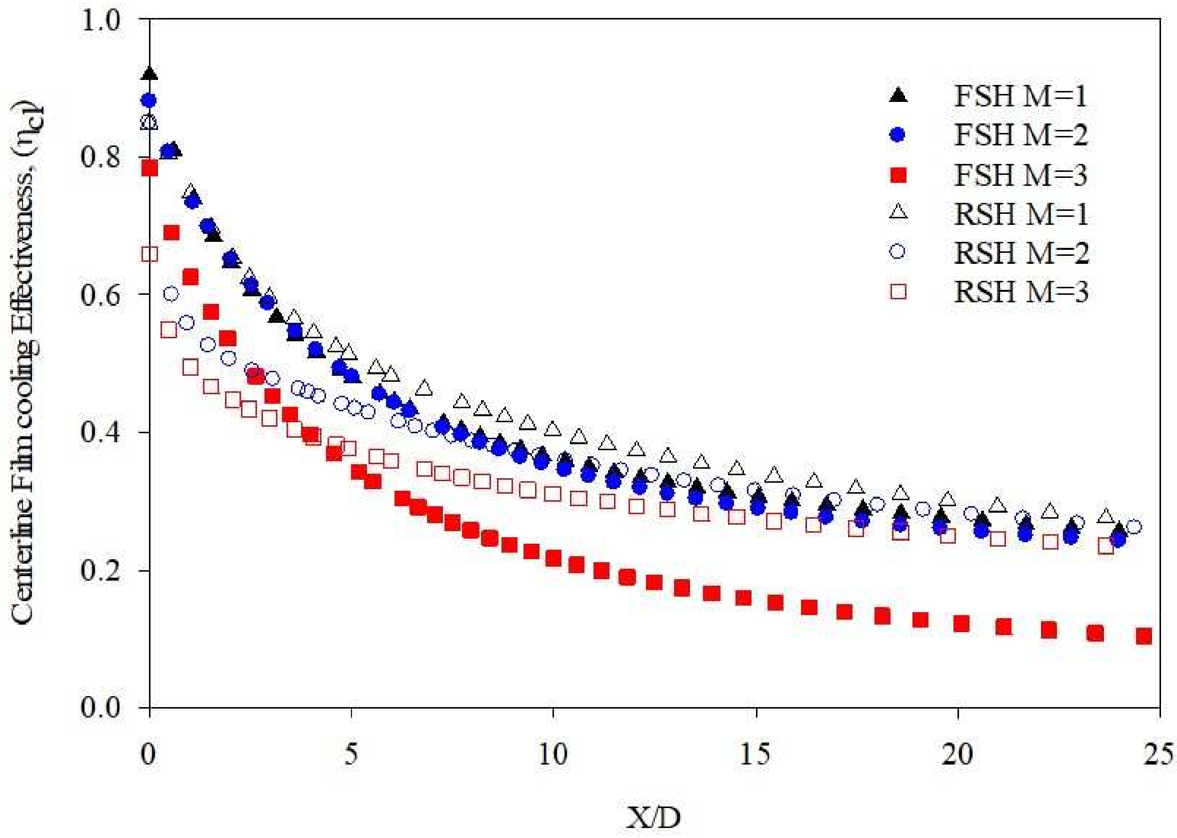

Fig. 7 comparison of centerline film cooling effectiveness with X/D for the FSH & RSH hole at different blowing ratios.

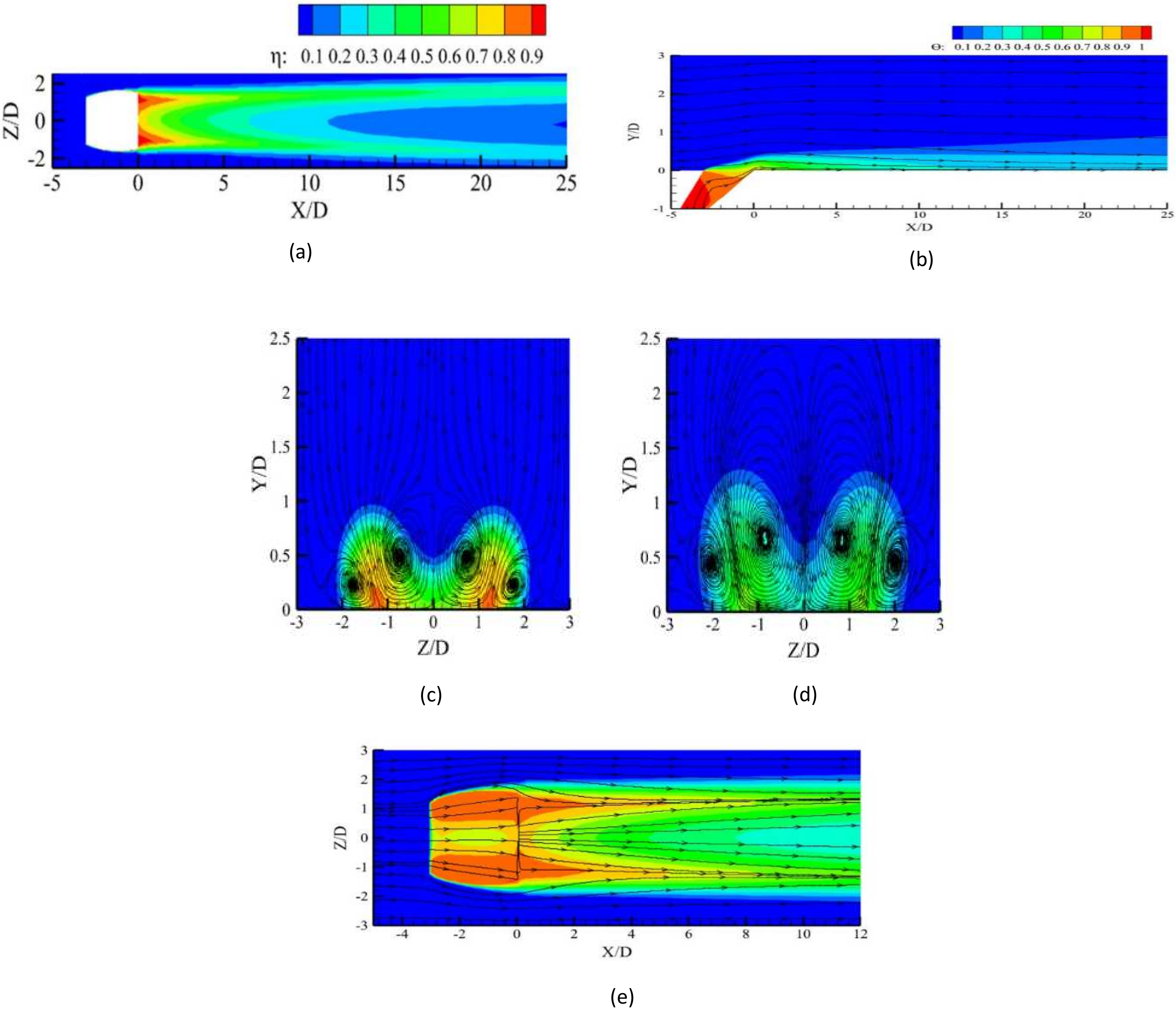

Fig. 8 FSH streamlines colored at M=2 (a) effectiveness downstream at Y/D = 0 (XZ Plane); dimensionless temperature(θ): (b) Z = 0 (XY plane), (c) X/D = 2 (YZ Plane), (d) X/D =10 (YZ Plane) and, (e) Y/D = 0 (XZ Plane).

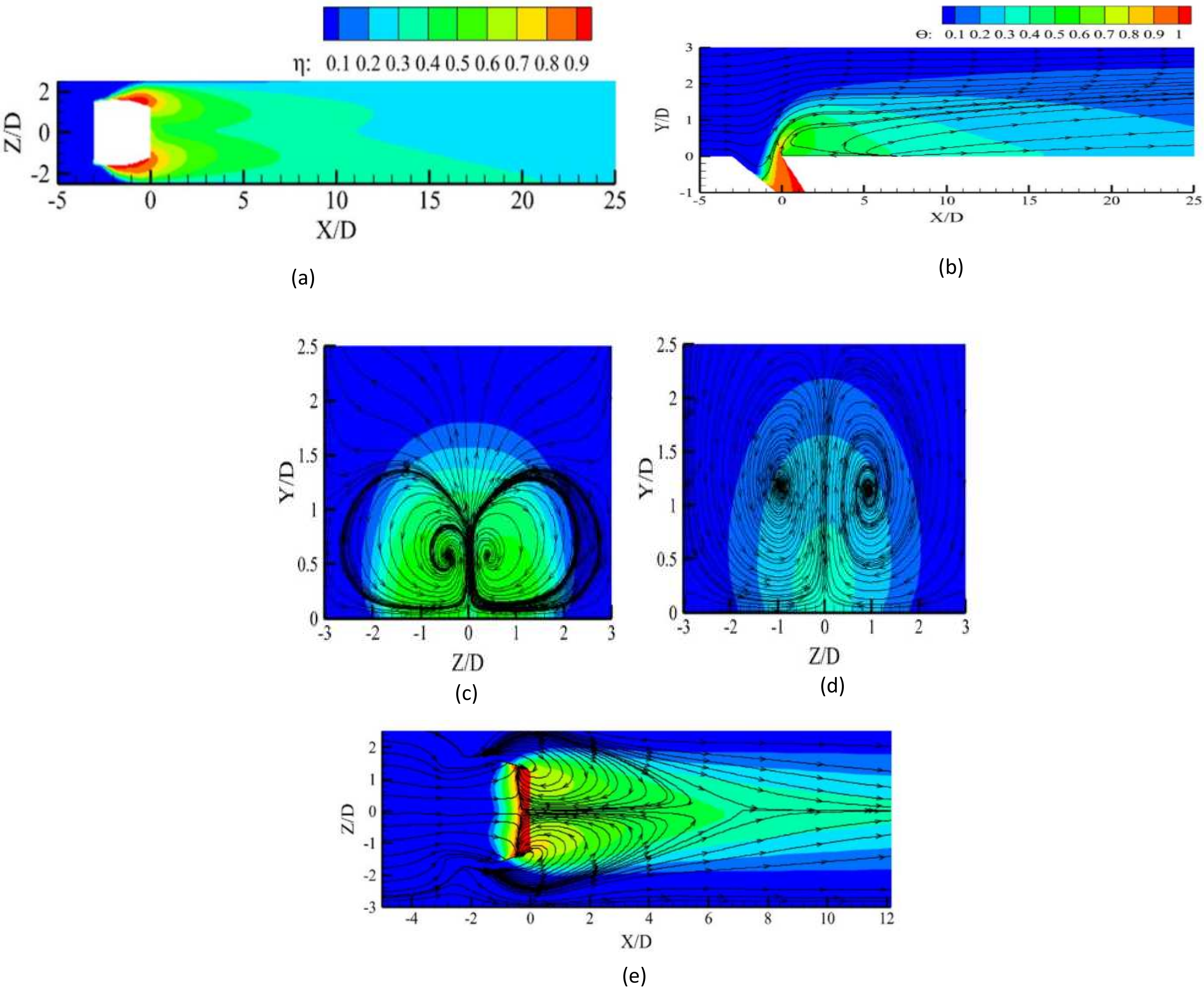

Fig. 9 RSH streamlines colored at M=2 (a) effectiveness downstream at Y/D =0 (XZ Plane); dimensionless temperature(θ): (b) Z = 0 (XY plane), (c) X/D =2 (YZ Plane), (d) X/D =10 (YZ Plane), and (e) Y/D = 0 (XZ Plane).

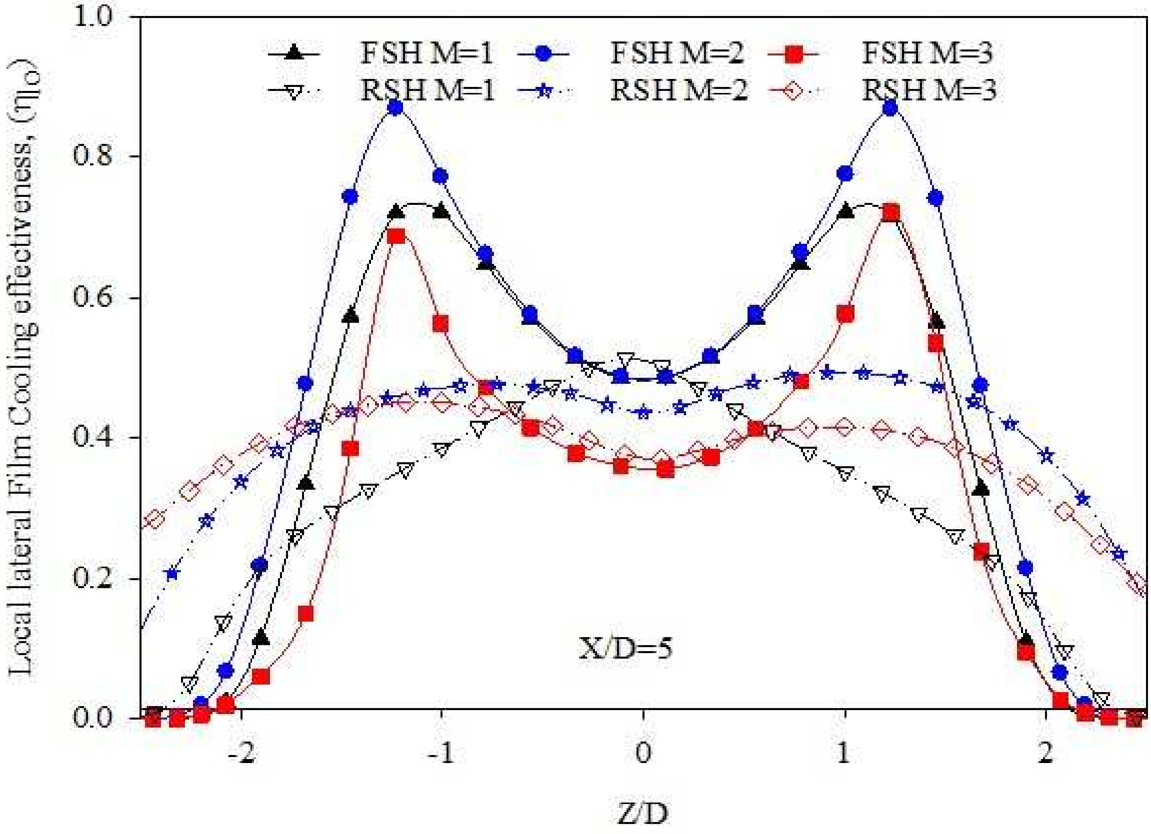

Fig. 10 Comparison of Local lateral film cooling effectiveness with X/D for the FSH and RSH hole at various blowing ratios.

Mr. Raj Gaurav is a research scholar in the Department of Mechanical Engineering at National Institute of Technology Manipur, Imphal West – Manipur, India. He obtained his Bachelor of Technology in Mechanical Engineering from National Institute of Technology Manipur, India in the year 2019. His topic of research is mist film cooling.

Mr. Ashutosh Kumar Singh is a Trainee Teacher in the Department of Mechanical Engineering at NIT Manipur. He received his bachelor's degree in Mechanical Engineering with University Gold-Medal in academics from Giani Zail Singh PTU Campus Bathinda Punjab in 2015 and selected by MHRD for NIT-IIT Trainee Teacher Scheme in 2016. He did Master's degree in Mechanical Engineering (Specialization: Fluids and Thermal Engineering) from Indian Institute of Technology Guwahati, Assam, 2018 and Currently pursuing his Ph.D. from Department of Mechanical Engineering, Indian Institute of Technology, Guwahati, Assam.

Dr. Kuldeep Singh is currently working in the Rolls Royce's University Technological Centre in "Gas Turbine and Transmission Research Centre (G2TRC), University of Nottingham, United Kingdom as a senior researcher. He has worked with the diverse team of international researchers. He is a Gold Medalist in B.Tech. He did M.Tech and PhD from IIT Delhi. He was Post-Doctoral Fellow in University of Beira Interior, Portugal. He is recipient of prestigious INSPIRE Faculty Award in 2017 from DST. He has worked on numerous projects sponsored by DRDO, DST, BHEL, Portuguese Foundation of Science and Technology, European Union & RR.

Dushyant Singh is an Associate Professor in the Department of Mechanical Engineering at Dr B R Ambedkar National Institute of Technology Jalandhar, Punjab- India. He finished his Doctorate's Degree in Mechanical Engineering from Indian Institute Technology, Delhi in 2014. He was postdoctoral researcher in joint research industrial project work with BHEL industry in IIT Delhi. He had been a faculty member in the Department of Mechanical Engineering at National Institute of Technology Manipur, India. His research interests include experimental and computational fluid flow – heat transfer, turbulence and two-phase heat transfer enhancement.